Progress In Electromagnetics Research, Vol. 136, 43–59, 2013

RADIATION ANALYSIS OF LARGE ANTENNA ARRAY BY USING PERIODIC EQUIVALENCE PRINCIPLE ALGORITHM

Kaizhi Zhang, Jun Ouyang*, Feng Yang, Chuan Wu, Yan Li, and Jian Zhang

School of Electronic and Engineering, University of Electronic Technology of China, China

Abstract—In this paper, an improved equivalence principle algorithm is proposed to solve the radiation problems of large antenna arrays with periodic structures. This method is a hybridization in which the typical scheme of periodic Green's function is combined with the original equivalence principle algorithm. The repeated elements are changed from the original antenna units into the surfaces enclosing the original ones. The proposed approach is compared with periodic method of moments which is based on the integral equation and the periodic Green's function. Numerical results validate the feasibility of the improved method.

1. INTRODUCTION

The research on large arrays with periodic structure, such as FSS (Frequency selective surface) [1, 2] and large antenna array [3, 4], has received much attention in recent years. In practical applications, such as the radiation problems of large antenna array, the results of radiation pattern cannot be calculated directly by principle of pattern multiplication. The interactions of the elements in the array should be considered. In order to simulate the currents on the element and the coupling among different elements accurately, full-wave method is necessary. Common numerical methods to solve the problems of antenna arrays include method of moments (MOM) [5–7], finite element method (FEM) [8], and finite difference time domain (FDTD) [9, 10]. MOM is based on integral equations. FEM and FDTD

Received 5 November 2012, Accepted 28 December 2012, Scheduled 16 January 2013
* Corresponding author: Jun Ouyang (antenna_ou@163.com).

are based on differential-equation-solver. However, the computational costs of the common numerical methods, such as the CPU time and memory requirement, will be large if many elements are placed in the array. Moreover, when the element consists of high permittivity and fine structures, some parts of mesh are denser than the other parts. Hence, the iterative solver will work in low efficiency for the multi-scale feature.

To estimate the characteristics of the array efficiently, numerical methods with periodic boundaries are involved [11–13]. Periodic method of moments (PMM) based on periodic Green's function [14–21] is a typical technique to evaluate infinite array. When utilizing the method to compute the radiation of a periodic array, repeated evaluations of the Green's function series are required to fill the impedance matrix [14]. Nevertheless, it is time consuming for the slow convergence rate of the series [15]. Several acceleration techniques are proposed to improve the convergence rate of the periodic Green's function by using the spectral and spatial formulations in conjunction with Poisson's and Shank's transformations[1, 18]. However, as the number of unknowns increases, the number of times to calculate the periodic Green's function will still increase correspondingly.

If the scale of impedance matrix becomes smaller, which means unknowns become fewer, the number of times to compute the periodic Green's function will decreases. This will lead the reduction of computational time. Equivalence principle algorithm (EPA) which bases on surface equivalence principle and domain decomposition method (DDM) is introduced in [22–28]. In this algorithm, virtual surfaces are utilized to enclose the sub-regions and translate the unknowns on objects to the unknowns on equivalence surfaces [18, 24, 28]. When complex structures, fine structures, or high permittivity dielectrics are involved in this problem, the density of unknowns on equivalence surfaces is much smaller than that on original objects [22]. Thus, EPA can reduce the number of unknowns and save computational costs. If the structures in elements are identical, the equivalence principle operator only needs to be calculated and stored once [25]. Besides, EPA can improve the conditioning of the impedance matrix whose elements are calculated by integral equations, so the number of iteration will be less than MOM [26].

By considering the characteristics of EPA and the advantages of the periodic Green's function, the periodic equivalence principle algorithm (PEPA) is proposed. In this method, the periodic Green's function is introduced into the original EPA. The proposed approach can reduce the number of unknowns through EPA. Therefore, the computational efficiency will be improved. Furthermore, when media

is involved, the problem of volume can be transformed into the problem of surface since the analysis task of EPA is to calculate the electrical and magnetic currents on the virtual surface. Moreover, in PEPA the problem inside the surface is unrelated to the periodicity since the periodicity is considered when computing the coupling of different surfaces. Therefore, the object inside can be changed in the range of the surface. The recalculation of the periodic Green's function will be avoided. More arrays with different sorts of element but same periodicity can be investigated efficiently.

In this paper, PEPA is utilized to solve the problems of large antenna array. The periodic Green's function is introduced when considering the coupling among different surfaces which enclose the antenna elements. The far field is evaluated by the electrical and magnetic currents on the surfaces. Numerical results reveal the feasibility of the proposed method.

2. PERIODIC GREEN'S FUNCTION

In this section, the periodic Green's function and periodic method of moments (PMM) are introduced briefly. The technique is mature, and applied widely in electromagnetic analyses of periodic structures. Consider a doubly periodic structure shown in Fig. 1. The elements in the infinite array are arranged in horizontal rows parallel to the x axis with spacing D_x, and the distance between the rows are D_y. The Green's function of the array can be written as a spatial series

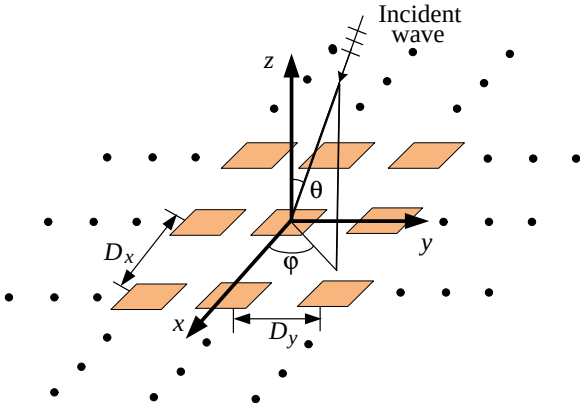

Figure 1. Geometry of an infinite array with doubly periodicity.

following [1, 21]:

$$G_P(\mathbf{r},\mathbf{r}') = \frac{1}{4\pi}\sum_{m=-\infty}^{\infty}\sum_{n=-\infty}^{\infty}\frac{e^{ikR_{mn}}}{R_{mn}}e^{j\phi_{mn}} \tag{1}$$

where,

$$R_{mn} = \sqrt{(xx'-x_{mn})^2+(y-y'-y_{mn})^2+z^2} \tag{2}$$

$$\phi_{mn} = k(x_m\sin\theta\cos\varphi + y_n\sin\theta\sin\varphi) \tag{3}$$

$\mathbf{r}\{=x,y,z\}$ represents the field point and $\mathbf{r}'\{=x',y',z'\}$ denotes the source points. $x_m = md_x$ and $y_n = nd_y$ are the coordinates of the elements in the structure. θ and φ are the angle of incident wave. k is the wave number in free space.

Periodic method of moments (PMM) is an actual application of periodic Green's function. In PMM, the periodic Green's function is used to substitute the Green's function in free space in method of moments (MOM) and enforce the periodic boundary conditions [14, 19]. Therefore, the electrical field integral equation (EFIE) in PMM can be represented as:

$$\mathbf{E}^{sca} + \mathbf{E}^{inc} = 0 \tag{4}$$

where,

$$\mathbf{E}^{sca} = i\eta k\int\left(\mathbf{J}G_p + \frac{1}{k^2}\nabla'\cdot\mathbf{J}\nabla G_p\right)d\tau' \tag{5}$$

$$\nabla G_p = \frac{1}{4\pi}\sum_{m=-\infty}^{\infty}\sum_{n=-\infty}^{\infty}(ikR_{mn}-1)\frac{\mathbf{R}_{mn}}{R_{mn}^3}e^{ikR_{mn}}e^{i\phi_{mn}} \tag{6}$$

η is the wave impedance in free space. G_p is the periodic Green's function. $\mathbf{J}$ is the currents in the periodic unit cell. Equation (6) is the gradient of the periodic Green's function [16]. The equations are tested in Galerkin's scheme. It is known that the series shown in (1) converge slowly. Mature methods are proposed to speed up the convergence. Methods based on Poisson summation are other effective ways to accelerate the convergence [1, 14, 16] by changing the spatial periodic Green's function into spectral form. The spectral form of the periodic Green's function can be written in Equation (7).

$$G_p(\mathbf{r},\mathbf{r}') = \sum_{m=-\infty}^{\infty}\sum_{n=-\infty}^{\infty}\frac{e^{-jk_x^{m,n}(x-x')}e^{-jk_y^{m,n}(y-y')}e^{-jk_z^{m,n}(z-z')}}{2jk_z^{m,n}D_xD_y} \tag{7}$$

where,

$$k_x^{m,n} = \frac{2\pi m}{D_x} + k_x^i = \frac{2\pi m}{D_x} + k_0 \sin\theta_i \cos\phi_i \tag{8}$$

$$k_y^{m,n} = \frac{2\pi n}{D_y} + k_y^i = \frac{2\pi m}{D_y} + k_0 \sin\theta_i \sin\phi_i \tag{9}$$

$$k_z^{m,n} = \begin{cases} \sqrt{k_0^2 - \left((k_x^{m,n})^2 + (k_y^{m,n})^2\right)}, & k_0^2 > (k_x^{m,n})^2 + (k_y^{m,n})^2 \\ -j\sqrt{\left((k_x^{m,n})^2 + (k_y^{m,n})^2\right) - k_0^2}, & k_0^2 < (k_x^{m,n})^2 + (k_y^{m,n})^2 \end{cases} \tag{10}$$

The gradient of the periodic Green's function in spectral domain can be expressed as following [16]:

$$\begin{aligned} &\nabla' G_p(\mathbf{r}, \mathbf{r}') \\ &= \sum_{m=-\infty}^{\infty} \sum_{n=-\infty}^{\infty} \frac{e^{-jk_x^{m,n}(x-x')} e^{-jk_y^{m,n}(y-y')} e^{-jk_z^{m,n}(z-z')}}{2jk_z^{m,n} D_x D_y} \\ &\cdot (jk_x^{m,n} e_x + jk_y^{m,n} e_y + jk_z^{m,n} e_z) \end{aligned} \tag{11}$$

Further, the terms of periodic Green's function can be reduced with enough accuracy by Ewald method mentioned in [1, 21].

3. EQUIVALENCE PRINCIPLE ALGORITHM

In EPA, objects are divided into several parts and each one is enclosed by a virtual surface called equivalence surface. The method includes two main procedures [22]: the scattering of objects via an

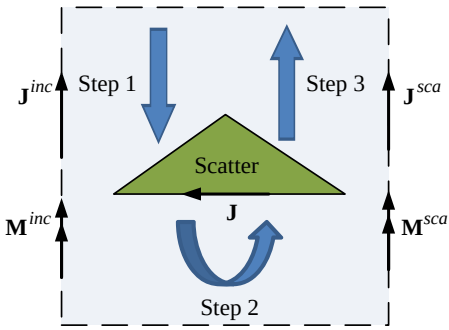

Figure 2. The procedure depicted by S operator. Step 1: outside-in propagation. Step 2: solving currents on the scatter. Step 3: inside-out propagation.

equivalence surface and the interaction among the different equivalence surfaces, are described by the equivalence operator (S operator) and the translation operator (T operator) respectively.

The procedure depicted by S operator includes three steps [24, 25]: outside-in propagation, solving currents on object, and inside-out propagation as shown Fig. 2. It is assumed that one scatter is enclosed by a virtual surface (the dashed).

The detailed description of S operator can be written as Equation (12). The unknowns on the object inside the surface can be transformed to the unknowns on the surface by S operator. This procedure can be described in Equation (13). $\mathbf{J}^{inc}$ and $\mathbf{M}^{inc}$ are the equivalence incident currents induced by the original source outside according to the equivalence principle. In the step one, the field generated by $\mathbf{J}^{inc}$ and $\mathbf{M}^{inc}$ only exists inside and it can be considered as the incident field of the scatter. In the step two, after the excitation of the scatter is obtained, the currents $\mathbf{J}$ on the scatter can be calculated easily by MOM. In the step three, the equivalence scattering currents $\mathbf{J}^{sca}$ and $\mathbf{M}^{sca}$ can be evaluated by $\mathbf{J}$ through the equivalence principle.

$$S = \begin{bmatrix} \mathbf{n}_e \times K \\ -\mathbf{n}_e \times L \end{bmatrix} [L_{obj}]^{-1} \begin{bmatrix} -\eta L & \eta K \end{bmatrix} \tag{12}$$

$$\begin{bmatrix} \mathbf{J}^{sca} \\ \frac{1}{\eta}\mathbf{M}^{sca} \end{bmatrix} = S \cdot \begin{bmatrix} \mathbf{J}^{inc} \\ \frac{1}{\eta}\mathbf{M}^{inc} \end{bmatrix} \tag{13}$$

$$\begin{aligned} K &= \frac{1}{4\pi} \int \nabla G \times \mathbf{X} d\tau \\ L &= \frac{ik}{4\pi} \int \left[\bar{\bar{I}} + \frac{1}{k^2} \nabla (\nabla \cdot \mathbf{X}) \right] G d\tau \end{aligned} \tag{14}$$

where K and L are the integral operators. G and η represent Green's function and wave impedance in free space. $\mathbf{n}_e$ denotes the outer normal vector of the surface.

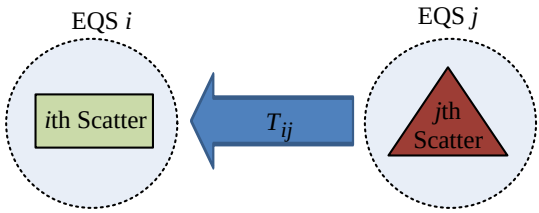

Figure 3. The interaction between the EQS i and EQS j.

The procedure of the interaction between the ith equivalence surface (EQS i) and the jth one (EQS j) shown in Fig. 3 can be described by translation operator or T operator as defined as following [23]:

$$\begin{bmatrix} \mathbf{J}_i \\ \frac{1}{\eta}\mathbf{M}_i \end{bmatrix} = \begin{bmatrix} \mathbf{n}_i \times K & \mathbf{n}_i \times L \\ -\mathbf{n}_i \times L & \mathbf{n}_i \times K \end{bmatrix} \begin{bmatrix} \mathbf{J}_j \\ \frac{1}{\eta}\mathbf{M}_j \end{bmatrix} = T_{ij} \begin{bmatrix} \mathbf{J}_j \\ \frac{1}{\eta}\mathbf{M}_j \end{bmatrix} \tag{15}$$

Finally, the EPA equations of the problem with N equivalence surfaces can be written as following:

$$\begin{bmatrix} I & -S_{11}T_{12} & \dots & -S_{11}T_{1N} \\ -S_{22}T_{21} & I & \dots & -S_{22}T_{2N} \\ \vdots & \vdots & \ddots & \vdots \\ -S_{NN}T_{N1} & -S_{NN}T_{N2} & \dots & I \end{bmatrix} \begin{bmatrix} C_1^s \\ C_2^s \\ \vdots \\ C_N^s \end{bmatrix} = \begin{bmatrix} V_1^{inc} \\ V_2^{inc} \\ \vdots \\ V_N^{inc} \end{bmatrix} \tag{16}$$

where I is identity operator. S_{ii} represents the S operator of ith surface. C_i^s is the coefficients of the equivalence scattering currents on the ith surface and V_i^{inc} is the excitation of the surface. If the elements in the array are identical, the S operator needs to be calculated and stored only once.

$$C_i^s = \begin{bmatrix} \mathbf{J}_i^{sca} \\ \frac{1}{\eta}\mathbf{M}_i^{sca} \end{bmatrix} \tag{17}$$

$$V_i^{inc} = S_{ii} \begin{bmatrix} \mathbf{J}_i^{inc} \\ \frac{1}{\eta}\mathbf{M}_i^{inc} \end{bmatrix} \tag{18}$$

4. PERIODIC EQUIVALENCE PRINCIPLE ALGORITHM

When utilizing the periodic method of moments (PMM) to solve the problem of infinite array, currents on only one unit cell will be considered. But when the cell has large number of unknowns, for example, fine structures, complicated structures, or high permittivity, PMM will be time-consuming since the number of times to evaluate the periodic Green's function series increases.

In order to solve the problem in this case, periodic equivalence principle algorithm (PEPA) which is a scheme combining the periodic Green's function with EPA is considered. This combination has several advantages. First, filling impedance matrix with periodic Green's function is the most time-consuming procedure in PMM. The number of unknowns can be reduced by EPA through transferring the unknowns on the object to the ones on the surface. The unknown density of surface is smaller than that on object. Hence, the number

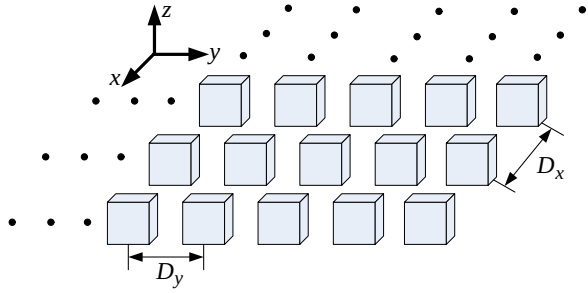

Figure 4. The equivalence surface array in PEPA. D_x and D_y are the distance between the two surfaces along x axis and y axis respectively.

of times for evaluating the periodic Green's function will decrease. Second, because the periodic Green's function is used on the virtual surface rather than the object, the periodicity will be not considered anymore when evaluating the currents on the object which involves the problem of volume-surface. The problem will be simplified. Third, the problem inside the surface is unrelated to the periodicity. Therefore, the object can be changed in the range of the surface and more arrays with different kinds of element but same periodicity can be investigated efficiently.

Like PMM, each periodic cell unit in PEPA should be identical. However, the unit cell is no longer the object but the equivalence surface enclosing the object. One infinite array is shown in Fig. 4 and each element is enclosed by a surface. As explained before, in EPA, the equivalence scattering currents $\mathbf{J}^{sca}$ and $\mathbf{M}^{sca}$ on one surface are determined by the currents of the inside scatter and the equivalence scattering currents on the other surfaces. When the array expands to the infinite one, the Equation (16) should be rewritten as following:

$$\begin{bmatrix} I & -S_{11}T_{12} & \dots & -S_{11}T_{1N} & \dots \\ -S_{22}T_{21} & I & \dots & -S_{22}T_{2N} & \dots \\ \vdots & \vdots & \ddots & \vdots & \dots \\ -S_{NN}T_{N1} & -S_{NN}T_{N2} & \dots & I & \dots \\ \vdots & \vdots & \dots & \vdots & \dots \end{bmatrix} \begin{bmatrix} C_1^s \\ C_2^s \\ \vdots \\ C_N^s \\ \vdots \end{bmatrix} = \begin{bmatrix} V_1^{inc} \\ V_2^{inc} \\ \vdots \\ V_N^{inc} \\ \vdots \end{bmatrix} \tag{19}$$

Obviously, for arbitrary i or j, $C_i^s = C_j^s$, $V_i^{inc} = V_j^{inc}$ (it is assumed that the amplitudes and the phases of the excitations are identical) and $S_{ii} = S_{jj}$ for the periodicity of the array. Therefore, the Equation (19) can be simplified as following:

$$[I - (S_{11}T_{12} + \ldots + S_{11}T_{1N} + \ldots)]\,[C_1^s] = \left[V_1^{inc}\right] \tag{20}$$

Further,

$$[I - S_{11}(T_{12} + \ldots + T_{1N} + \ldots)]\,[C_1^s] = \left[V_1^{inc}\right] \tag{21}$$

Then, the sum of the translation operators can be replaced by a periodic translation operator (T_P operator) as following:

$$T_P = \begin{bmatrix} \mathbf{n}_e \times K_P & \mathbf{n}_e \times L_P \\ -\mathbf{n}_e \times L_P & \mathbf{n}_e \times K_P \end{bmatrix} \tag{22}$$

where,

$$\begin{aligned} K_P &= \frac{1}{4\pi} \int \nabla G_P \times \mathbf{X} d\tau \\ L_P &= \frac{ik}{4\pi} \int [\bar{\bar{I}} + \frac{1}{k^2} \nabla(\nabla \cdot \mathbf{X})] G_P d\tau \end{aligned} \tag{23}$$

The subscript P denotes periodicity. K_P and L_P are the integral operators with the periodic Green's function. $\mathbf{n}_e$ is the outer normal vector of the equivalence surface. G_P represents the periodic Green's function discussed in the section two.

5. NUMERICAL RESULTS

In this section, four examples are utilized to investigate the accuracy and efficiency of PEPA. The currents are calculated by iterative solver GMRES. All results of programs are computed by the machine with CPU of AMD Atholon II $\times 4$ and memory of 8 GB.

First, in order to demonstrate the correctness of PEPA, RCS of one PEC ball array is investigated. The model is shown in Fig. 5(a). The scale of the array is 51×51. D_x and D_y which are the spacing between two balls along x axis and y axis both equal $1\lambda_0$. λ_0 is the wavelength in free space. The radius of each ball is 0.3 m. The incident plane wave propagates along the direction paralleling z axis. The frequency is 300 MHz. Each ball is enclosed by a virtual spherical surface. The radius of the surface is 0.4 m. The unknowns of PEC ball is 342 and the unknowns of the surface is 729. RWG basis function is used to simulated the currents on the balls and surfaces. The RCS values of MOM in FEKO, PMM and PEPA are compared in Figs. 5(b) and (c). RCS from FEKO is the precise result of calculating a finite array with 51×51. The forms of periodic Green's function of PMM and PEAP are identical. The accuracy of PMM is acceptable in the range of $0 \sim 45°$, $135° \sim 215°$ and $315° \sim 360°$. Errors appear at range around $90°$ since PMM is an asymptotical method which considers that the currents on each element are same. Differences between currents at the edge of the array and those in the center are neglected. The method can be

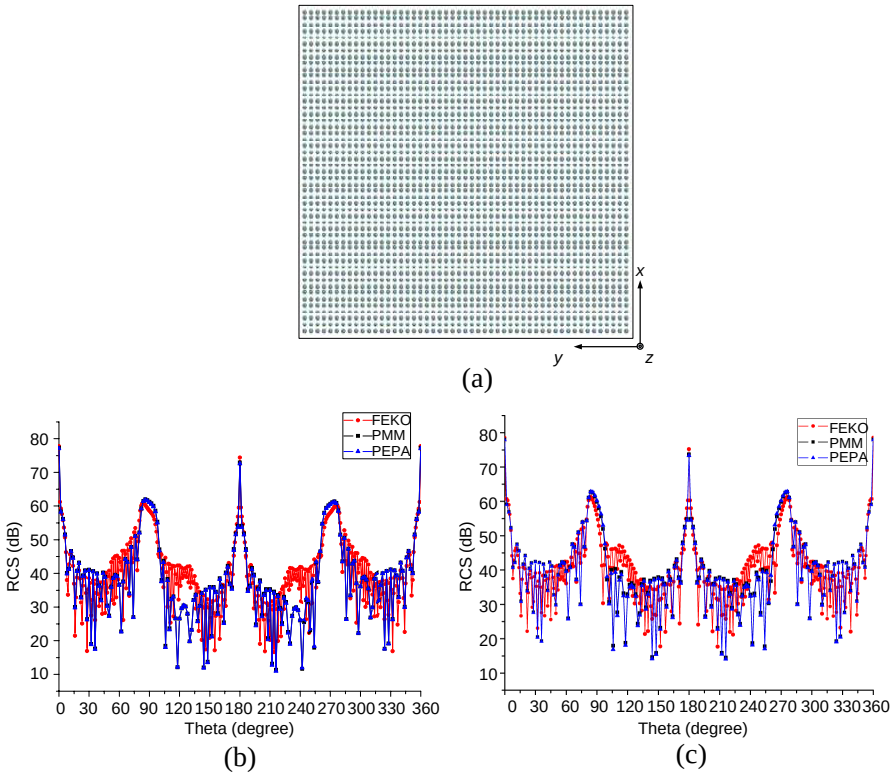

Figure 5. (a) The model of 51×51 ball array. $D_x = D_y = 1\lambda_0$. (b) RCS of 51×51 ball array (HH). (c) RCS of 51×51 ball array (VV).

Table 1. The comparison of computational efficiency between PMM and PEPA.

	PMM	PEPA
CPU time	9 hours and 17 minutes	2 hours and 47 minutes

competent to mission on the radiating estimation of arrays. On the other hand, PMM and PEPA have a good agreement. Therefore, the transformation from PMM to PEPA is feasible.

Second, the radiation pattern of one large antenna array is discussed. The comparison of PMM and PEA about the computational efficiency is revealed. Fig. 6(a) shows a microstrip antenna array with the scale of 101×101. Each antenna works at 4 GHz. The thickness of

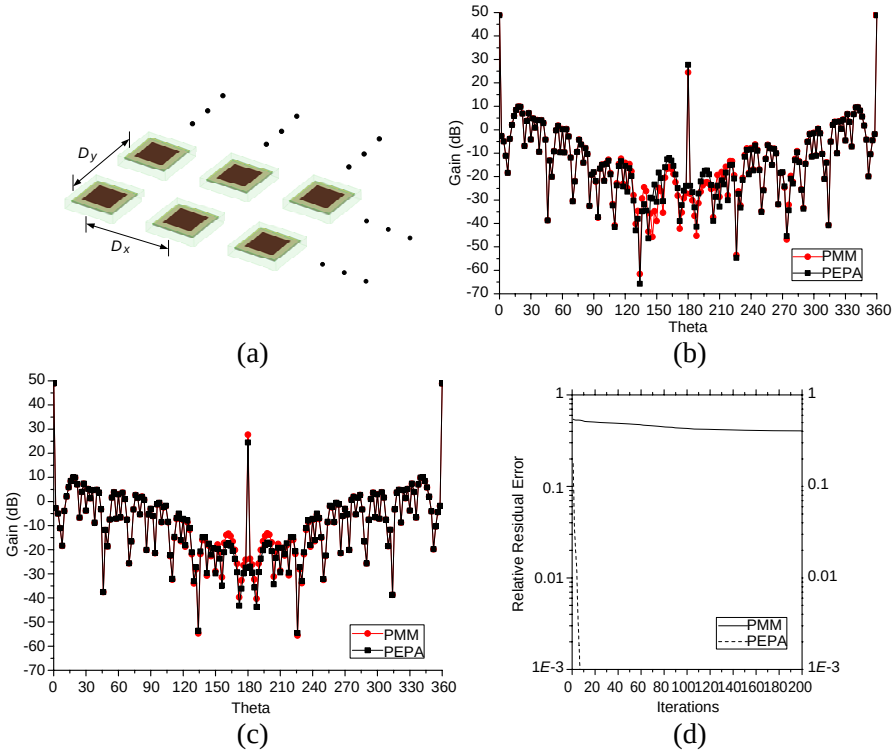

Figure 6. (a) Model of 101×101 microstrip antenna array. (b) E-plane pattern (Phi = 0°). (c) H-plane pattern (Phi = 0°). (d) The comparison of iterations between PMM and PEPA.

the substrate is about $0.027\lambda_0$. ε_r is 2.2 and μ_r is 1.0. The unknowns is 3020 for each element which is enclosed by a virtual surface with the scale of $0.80\lambda_0 \times 0.80\lambda_0 \times 0.44\lambda_0$. λ_0 is the wavelength in free space. The unknowns on the virtual surface is 612×2 (equivalence electrical currents and equivalence magnetic currents). Obviously, the unknown reduction in PEPA is about 59%. The volume-surface integral equation (VSIE) [29] is utilized solve the currents on the elements. The basis-functions in this problem include RWG basis and SWG basis. The distance between two antennas is $0.9\lambda_0$ long x axis (D_x) and $0.9\lambda_0$ long y axis (D_y). For simplifying the problem, the excitations are identical in amplitude and phase. The radiation simulation of the antenna array is shown in Figs. 6(b) (c) and the efficiency comparison is revealed in Table 1. Obviously, the efficiency of PEPA is higher than PMM in this problem. The phenomenon can be explained as following:

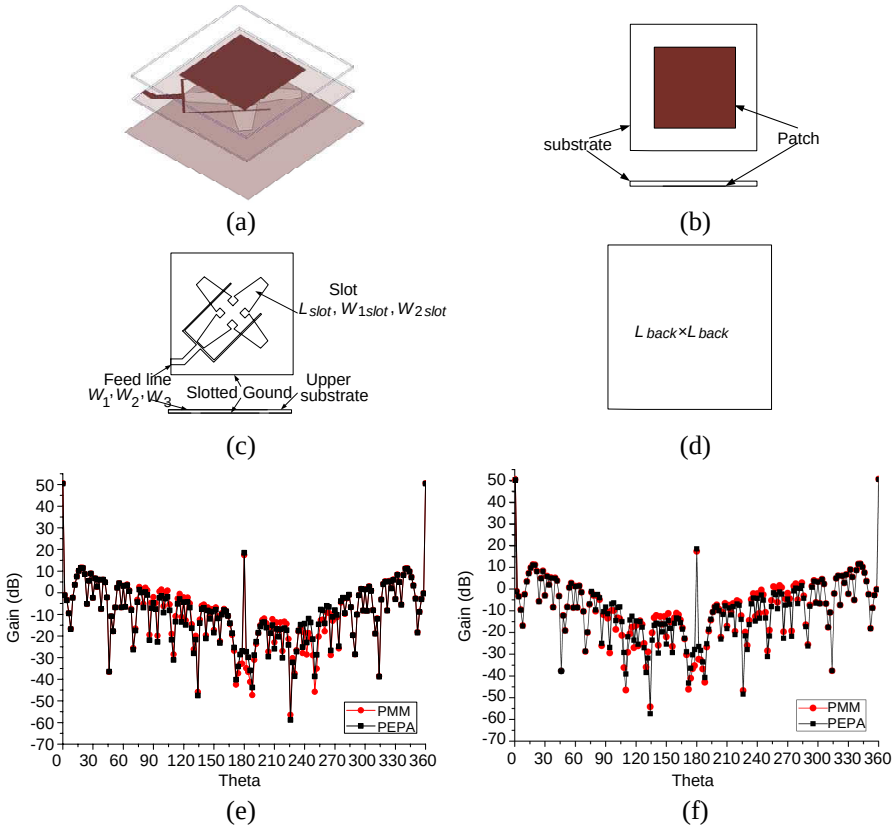

Figure 7. (a) The model of the antenna element. (b) Upper layer of the element. (c) Middle layer of the element. (d) Back board. (e) Radiation pattern of E plane. (f) Radiation pattern of H plane.

firstly, unknowns in PEPA is fewer than PMM, which means the scale of impedance matrix with the periodic Green's function is smaller than that in PMM. So, the number of times to evaluate the series becomes less. Secondly, the convergence rate of PEPA illustrated in (d) is faster than PMM since EPA can improve the conditioning of the impedance matrix.

Third, as mentioned before, the periodicity of the array is independent to the problem inside the virtual surface in PEPA, since the periodic Green's function is used only on the surface. Therefore, only S operator without the periodic Green's function series will need to be calculated again if another antenna array with same periodicity needs to be investigated. T operator can be reserved. In this example, the element in example two is changed into another one. The design of

Table 2. Value of all parameters of the feed structure.

L_{slot}	W_{1slot}	W_{2slot}	W_1	W_2	W_3	L_{back}
35.1 mm	4.1 mm	8.1 mm	2.0 mm	0.68 mm	0.34 mm	50.9 mm

Table 3. The comparison of computational efficiency between PMM and PEPA.

	PMM	PEPA
CPU time	21hours and 23 minutes	1 hours and 46 minutes

the element [30] is shown in Figs. 7(a) (b) (c) (d) and the parameters are shown in Table 2. The antenna is working at 4 GHz. The total number of the element is 4511. The surfaces are identical to the ones in example two including the size, positions and meshes. The radiation patterns are shown in (e) and (f). The computational efficiency is compared in Table 3. Based on the data of T operator in example two, the elapsed time of PEPA in this problem is much shorter than PMM in which the whole periodic Green's function series are recalculated. It is concluded that PEPA is competent to the estimation of radiation on antenna arrays with same periodicity but different elements.

Finally, an antenna array in one-dimension is investigated. In example two and three, arrays with large separation between elements have been considered. However, in many practical application, a separation distance of less than half wavelength is needed for suppressing the gating lobe. In this example, one 1D scanning array with 15 quasi-Yagi antennas is discussed. The model is shown in Fig. 8(a). The antenna works at 15 GHz. The lengths of director, driver and reflector are $0.17\lambda_0$, $0.43\lambda_0$ and $0.75\lambda_0$ respectively. The director is put $0.16\lambda_0$ above the driver and the reflector is put $0.31\lambda_0$ below the driver. The thickness of the substrate is about $0.032\lambda_0$. ε_r is 2.2 and μ_r is 1.0. The unknowns is 2590. Each element is enclosed by a virtual surface with the scale of $0.20\lambda_0 \times 0.90\lambda_0 \times 0.95\lambda_0$. λ_0 is the wavelength in free space. The unknowns of the equivalence surface is 732×2. The separation distance between two elements is $0.48\lambda_0$ along x axis (D_x). The amplitude of each excitation is identical and the phase difference of neighboring cell is 100°. The phase can be set in Equation (1). The accuracy of PMM and PEPA are compared with MOM in this application. The radiation simulation shown in Fig. 8(b) reveals that the accuracy of PMM is acceptable compared with MOM from FEKO in the range near the main lobe. The main lobe appears at 40° for the phase difference. However, errors appear near 90° for the reason of neglecting the difference of currents among the elements. The PMM and PEPA are in good agreement.

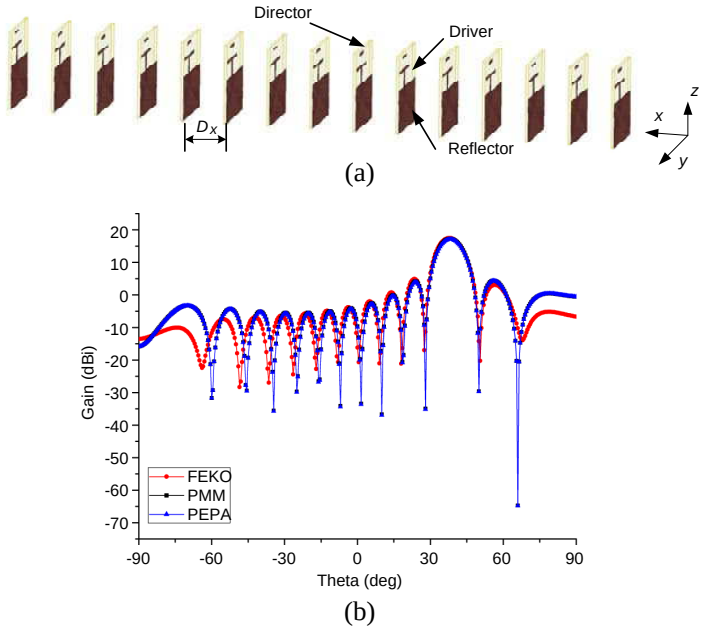

Figure 8. (a) The model of the scanning array. (b) The radiation pattern of H-plane.

6. CONCLUSION

In this paper, one improved EPA, in which the periodic Green's function is combined with the original EPA, is proposed to estimate the radiation of antenna arrays with large scale. The periodic Green's function is applied in the procedure of computing the interactions among different equivalence surfaces. The number of times to evaluate the periodic Green's function series is reduced due to the characteristic of EPA. Furthermore, the conditioning of the impedance matrix is also improved after EPA involved. The accuracy and high efficiency of PEPA is discussed. The numerical results demonstrate the feasibility of the proposed approach in the field of estimating the antenna array with large scale.

ACKNOWLEDGMENT

This work was supported by the postdoctoral Science Foundation of China (Nos. 20090461325 and 201003690), the Natural Science Foundation of China (No. 61001029), the Fundamental Research

Funds for the Central Universities (No. ZYGX2010X005), and the Aeronautical Science Foundation (No. 2011018001) and Key Laboratory of Advanced Integrated Electronic System, Ministry of Education, University of Electronic Science and Technology of China, Chengdu.

REFERENCES

1. Su, J. X., X. W. Xu, M. He, and K. Zhang, "Integral-equation analysis of frequency selective surfaces using Ewald transformation and lattice symmetry," *Progress In Electromagnetics Research*, Vol. 121, 249–269, 2011.
2. Zhang, J.-C., Y.-Z. Yin, and J.-P. Ma, "Design of narrow band-pass frequency selective surfaces for millimeter wave applications," *Progress In Electromagnetics Research*, Vol. 96, 287–298, 2009.
3. Wan, J. X., J. Lei, and C. H. Liang, "An efficient analysis of large-scale periodic microstrip antenna arrays using characteristic basis funciton method," *Progress In Electromagnetics Research*, Vol. 50, 61–81, 2005.
4. Peng, Z. and J.-F. Lee, "Non-conformal domain decomposition method with mixed true second order transmission condition for solving large finite antenna arrays," *IEEE Trans. Antenn. Propaga.*, Vol. 59, No. 5, Aug. 2011.
5. Xia, L., C.-F. Wang, L.-W. Li, P.-S. Kooi, M.-S. Leong, "Resonant behaviours of microstrip antenna in multilayered media: An efficient fullwave analysis," *Progress In Electromagnetics Research*, Vol. 31, 55–67, 2011.
6. La Cono, G., R. Gardelli, M. Albani, and A. Freni, "An efficient full-wave-MOM for RLSA antennas," *IEEE Antennas and Propagation Society International Symposium*, Vol. 3A, 118–121, Jul. 2005.
7. Lim, C.-P., "Method of moments analysis of electrically large thin square and rectangular loop antennas: Near-and-far-zone field," *Progress In Electromagnetics Research*, Vol. 34, 117–141, 2001.
8. Trujillo-Romero, C. J., L. Leija, and A. Vera, "FEM modeling for performance evaluation of an electromagnetic oncology deep hyperthermia applicator when using monopole inverted T, and plate antennas," *Progress In Electromagnetics Research*, Vol. 120, 99–125, 2011.
9. Lei, J.-Z., C.-H. Liang, W. Ding, and Y. Zhang, "EMC analysis of antennas mounted on electrically large platforms with parallel

FDTD method," *Progress In Electromagnetics Research*, Vol. 84, 205–220, 2008.

10. Yang, S.W., Y. K. Chen, and Z. P. Nie, "Simulation of time modulated linear antenna array using the FDTD method," *Progress In Electromagnetics Research*, Vol. 98, 175–190, 2009.
11. McGrath, D. T. and V. P. Pyati, "Periodic boundary conditions for finite element analysis of infinite phased array antennas," *IEEE Antenna and Propagation Society International Symposium*, Vol. 3, 1502–1505, 1994.
12. Mahachoklertwattana, P., P. H. Pathak, C.-F. Wang, and Y.-B. Gan, "A fast MOM solution for large finite planar periodic arrays with non-rectangular element truncation boundaries," *IEEE APMC*, 1–4, 2007.
13. Holter, H. and H. Steyskal, "Broadband FDTD analysis of infinite phased arrays using periodic boundary conditions," *Electronics Letters*, 758–759, 1999.
14. Barlevy, A. S. and Y. Rahmat-Samii, "Characteristics of electromagnetic band-gaps composed of multiple periodic tripods with interconnecting vias: Concept, analysis and design," *IEEE Trans. Antenn. Propaga.*, Vol. 49, No. 3, Mar. 2001.
15. Su, J., X. Xu, and M. He, "Hybrid PMM-MOM method for analyzing the RCS of finite array," *IEEE International Conference on Information Science and Technology*, 532–535, 2011.
16. Guerin, N., C. Craeye, and X. Dardenne, "Accelerated computation of the free space Green's function gradient of infinite phased arrays of dipoles," *IEEE Trans. Antenn. Propaga.*, Vol. 57, No. 10, Oct. 2009.
17. Dardenne, X. and C. Craeye, "Method of moments simulation of infinitely periodic structures combining metal with connected dielectric objects," *IEEE Trans. Antenn. Propaga.*, Vol. 56, No. 8, Aug. 2008.
18. Shubair, R. M. and Y. L. Chow, "Efficient computation of the periodic Green's function in layered dielectric media," *IEEE Trans. Antenn. Propaga.*, Vol. 41, No. 3, Mar. 1993.
19. Miura, A. and Y. Rahmat-Samii, "RF characteristics of spaceborne antenna mesh reflecting surfaces: Application of periodic method of moments," *IEEE Antenna and Propagation Society International Symposium*, Vol. 3A, 375–378, 2005.
20. Bahadori, H., H. Alaeian, and R. Faraji-Dana, "Computation of periodic Green's functions in layered media using complex images technique," *Progress In Electromagnetics Research*, Vol. 112, 225–

240, 2011.

21. Stevanovic, I. and J. R. Mosig, "Green's functions for planar structures in periodic skewed 2-D lattices using Ewald transformation," *IEEE EuCAP*, 1–6, 2006.
22. Li, M.-K. and W. C. Chew, "Wave-field interaction with complex structures using equivalence principle algorithm," *IEEE Trans. Antenn. Propaga.*, Vol. 55, No. 1, 130–138, Jan. 2007.
23. Sun, L.-E., M.-K. Li, and W. C. Chew, "Applying the low frequency technique to the equivalence principle algorithm," *Antenna and Propagation Society International Symposium*, 1–4, 2009.
24. Li, M. K. and W. C. Chew, "A domain decomposition scheme based on equivalence theorem," *Micro. Opt. Tech. Lett.*, Vol. 48, No. 9, 1853–1857, Sep. 2006.
25. Shao, H., J. Hu, Z. Nie, G. Han, and S. He, "Hybrid tangential equivalence principle algorithm with MLFMA for analysis of array structures," *Progress In Electromagnetics Research*, Vol. 113, 127–141, 2011.
26. Yla-Oijala, P. and M. Taskinen, "Solving electromagnetic scattering by large and complex structures with surface equivalence principle algorithm," *Waves in Random and Complex Media*, Vol. 19, No. 1, Feb. 2009.
27. Yla-Oijala, P. and M. Taskinen, "Solving electromagnetic scattering by multiple targets with surface equivalence principle algorithm," *3rd European Conference on Antenna and Propagation*, 88–92, Mar. 2009.
28. Li, M.-K. and W. C. Chew, "Multiscale simulation of complex structures using equivalence principle algorithm with high-order field point sampling scheme," *IEEE Trans. Antenn. Propaga.*, Vol. 56, No. 8, 2389–2397, Aug. 2008.
29. Ouyang, J., F. Yang, S. W. Yang, and Z. P. Nie, "Exact simulation method VSIE+MLFMA for analysis radiation pattern of probe-feed conformal microstrip antenna and the application of synthesis radiation pattern of conformal array mounted on finite-length PEC circular cylinder with DES," *Journal of Electromagnetic Waves and Applications*, Vol. 21, No. 14, 1995–2008, 2007.
30. Luo, W., S. Yang, and Z. Nie, "A wideband and dual polarization base station antenna for IMT-advanced system," *Cross Strait Quad-Regional Radio Science and Wireless Technology Conference*, Vol. 1, 483–486, 2011.